

An *ISO* view on interstellar dust heated by red giant stars^{*}

T. Le Bertre¹, G. Lagache², N. Mauron³, F. Boulanger², F.X. Désert², N. Epchtein¹, and P. Le Sidaner¹

¹ Observatoire de Paris, 61 av. de l'Observatoire, F-75014 Paris, France

² Institut d'Astrophysique Spatiale, Bat. 121, Université Paris Sud, F-91405 Orsay Cedex, France

³ ISTEEM, CNRS, Université de Montpellier II, cc072 Place Eugène Bataillon, F-34095 Montpellier Cedex 05, France

Received 5 January 1998 / Accepted 12 March 1998

Abstract. In order to study the structure and emission of the diffuse interstellar medium when it is heated by red giant stars, we have obtained *ISOPHOT* maps centered at proximity of a sample of such objects. The maps are $7' \times 7'$ with a pixel size of $45''$, and were made at 60 and $90 \mu\text{m}$. Here we present the preliminary results of this program, based on data from 11 fields recently achieved by *ISO*. The maps have been centered at $4.7'$ from the star but do not contain it to avoid saturation. In 7 cases out of 11 we observe an infrared emission with a gradient toward the star. This effect is most probably due to radiative heating of grains which closely surround the red giant, and not to foreground or background matter. The emission is structured at the level of the map pixel, i.e. $45''$, which corresponds to typical linear sizes of $\sim 0.1\text{--}0.3$ pc.

Key words: stars: individual: R Aqr – dust, extinction – ISM: general – infrared: ISM: continuum

1. Introduction

The large luminosity of Asymptotic Giant Branch (AGB) stars potentially makes them important heating sources of the Interstellar Medium (ISM) that surrounds them. The luminosities are in most cases between $5 \cdot 10^3$ and $2 \cdot 10^4 L_{\odot}$, which is comparable to those of B1-B2 main sequence stars. Interestingly, their spectra peak at wavelengths larger than $1 \mu\text{m}$, and, to the difference of early-type stars, they do not emit in the ultraviolet range. Therefore, they cannot contribute to the excitation of large molecules and very small grains (Désert et al. 1990), and the dominant effect is through radiative heating of the large grain component of the interstellar (IS) dust. In addition, they do not modify strongly the density structure of the ISM, except in the central cubic parsec, because of the low velocity of their winds (typically 15 km s^{-1} , as compared to $100\text{--}1000 \text{ km s}^{-1}$ for the other luminous stars).

Send offprint requests to: T. Le Bertre, (lebertre@obspm.fr)

^{*} Based on observations with *ISO*, an ESA project with instruments funded by ESA Member States (especially the PI countries: France, Germany, the Netherlands and the United Kingdom) and with the participation of ISAS and NASA

The heating effect by red giants has been described by Le Sidaner & Le Bertre (1993). They show that dust in the ISM around AGB stars should be heated up to distances of 1–2 pc. In the corresponding volume, the dust reaches temperatures in the range 30–50 K. Therefore, provided that IS dust is present, the effect should show up in the range 60–100 μm , and will be best seen if some imagery is made with sufficient angular resolution ($\leq 1'$ for fields at ~ 1 kpc).

We have undertaken an observing program with the *Infrared Space Observatory (ISO)*, Kessler et al. 1996) to study this effect. The observations consist of 9×9 maps acquired at 60 and $90 \mu\text{m}$ with the PHOT instrument (Lemke et al. 1996). The heating sources have been selected among a sample of nearby ($d \leq 2$ kpc) red giant stars. Our sample is not established rigorously, but the characteristics of the stars and of their envelopes are particularly well known and constrained by available data and previous work. The sources were chosen, also, to offer a large range of parameters such as the height above galactic plane or the peak wavelength of their spectrum.

By probing the ISM in various locations, our program will give new insights on the small scale structure, typically $\sim 0.1\text{--}0.4$ pc, and on the dust filling factor of the ISM. At the time of writing, the observations are still in progress. In this paper, we report on results based on the first eleven fields observed by *ISO*.

The observations and data processing are described in Sect. 2 and the results, in Sect. 3. A preliminary analysis of the data is given in Sect. 4.

2. Observations and data reduction

For the original (*ISO* pre-launch Call) observing program, we specified fields near sources chosen in the samples of well-studied carbon-rich (hereafter C-rich) AGB stars (Le Bertre 1992), and oxygen-rich (hereafter O-rich) AGB stars (Le Bertre 1993). Concerning the supplemental (post-launch) program, with consideration to pointing limitations, the same list was adopted and extended to include some new fields at proximity of other well documented nearby red giants. The fields which are actually observed are progressively selected in our lists by the *ISO* Operations Team at Villafranca, Spain.

Basic parameters concerning the fields discussed here are given in Table 1. Distances are adopted from Le Bertre (1997) for C-rich heating sources, and from Le Bertre & Winters (1998) for O-rich ones. The distance to μ Cep is adopted from Humphreys (1978). Finally, z is the distance to the galactic plane.

The data have been acquired with the C100 3×3 pixels array through filters C_60 and C_90. The pixel size on the sky is $43.5'' \times 43.5''$, and their separation (centre to centre), $\sim 46''$. The effective wavelengths of the filters C_60 and C_90 are respectively 61 and $95 \mu\text{m}$, and their half-maximum widths 24 and $50 \mu\text{m}$ (ISOPHOT Observer's Manual). The maps are obtained by asking *ISO* to make a 3×3 raster scan with no overlap, so that the final maps are composed of 9×9 pixels and have a size of $415'' \times 415''$. The integration time is 128 s for each pointing, so that the total integration time per field is 2304 s. As the orientation of the satellite on the sky depends on the global *ISO* scheduling, the images are acquired with an arbitrary orientation with respect to celestial coordinates. However, for all fields, the acquisitions of the 60 and $90 \mu\text{m}$ maps are linked in time so that they should overlay almost perfectly. Finally, to avoid saturation and remanence effects, the field centers were chosen to be offset from the red giant by $280''$ in declination so that the source is out of the map for any orientation.

Reduction of ISOPHOT data was performed with the version 6.1 of the PHOT Interactive Analysis (PIA¹) software starting from the raw data level (ERD). The calibration in flux was derived from the Fine Calibration Source (FCS) data bracketting the astronomical observations. The pattern of the 3×3 array was still visible in the pipeline processed maps. This effect has been corrected by a dedicated flatfielding of the individual maps. For that purpose, the low level flux regions of each map were selected. A flat field was derived by comparing the median flux of each individual pixel to the median of the 9 pixel fluxes. It was then applied to the PIA processed maps with satisfactory results.

Unfortunately, some doubts remain about the absolute calibration of the fluxes. At the present stage, we are confident in the relative fluxes inside each map, but not on their absolute levels. A better understanding of the characteristics of the C100 detector is required. For one of the pointings at $60 \mu\text{m}$ in the field near AFGL 3099, the data are missing.

3. Results

Figs. 1 and 2 show a representative example of the 60 and $90 \mu\text{m}$ maps obtained. The location of the *ISO* field with respect to the heating source is illustrated on Fig. 3.

A strong flux is generally found, but not always, on the pixels located nearest to the star. Naturally, any enhanced emission from the surrounding ISM near a red giant has to be distinguished from the general emission arising anywhere along the

¹ PIA is a joint development by the ESA Astrophysics Division and the ISOPHOT Consortium led by the Max Planck Institute for Astronomy (MPIA), Heidelberg. Contributing ISOPHOT Consortium institutes are DIAS, RAL, AIP, MPIK, and MPIA.

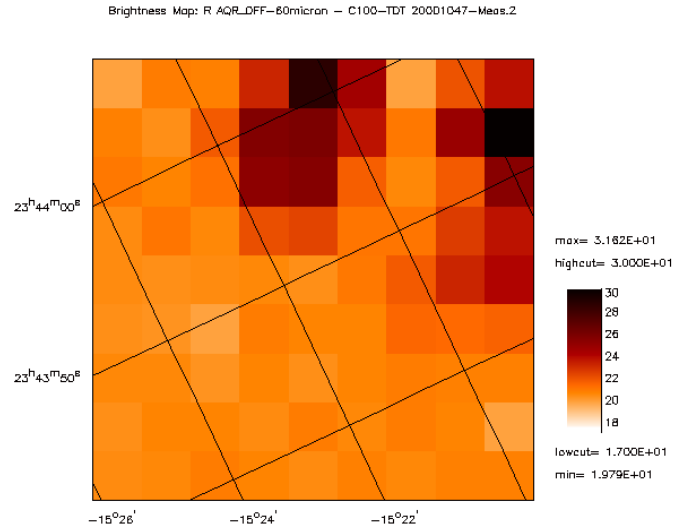


Fig. 1. Field near R Aqr at $60 \mu\text{m}$; the rotation angle w.r.t. celestial coordinates is 64.7° . North is to the upper right corner and East, to the upper left one. At 215 pc, the pixel corresponds to 0.045 pc . The heating source is outside the map, near the upper part of the right edge (see also Fig. 3)

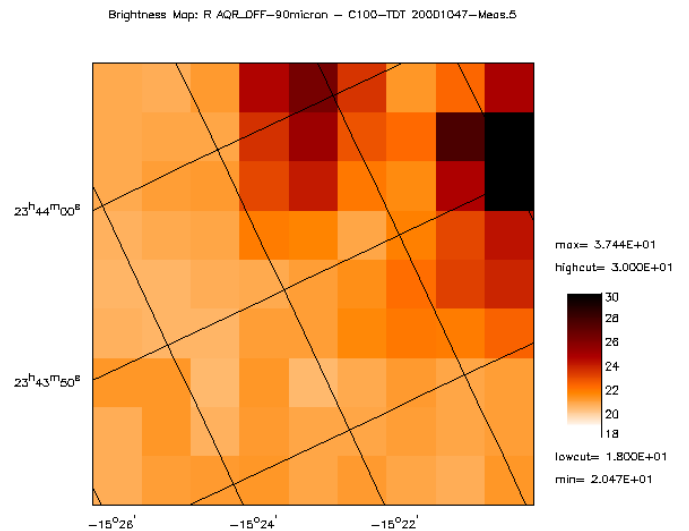


Fig. 2. Same as Fig. 1 at $90 \mu\text{m}$

line of sight. This difficulty can be overcome, at least partially, by looking at the map morphology and by searching flux gradients along radial directions to the heating source. In the R Aqr field, there is an obvious gradient and a strong flux contrast between the region located near the star, and the opposite region.

To evidence that effect, we have averaged the pixel fluxes within rings centered on the source position (assuming no error on the *ISO* positioning indications). The result is shown in Fig. 4 for the R Aqr field. A strong flux decrease is found in both bands. Table 2 lists the objects for which a gradient toward the heating source is detected with this procedure. The expected effect is found clearly in 6 cases out of 10. Concerning the field near AFGL 3099, it is difficult to make a similar firm conclusion

Table 1. Basic data

AGB heating source	dist. (pc)	z (pc)	field α (2000.0)	center δ (2000.0)	l^{II}	b^{II}	observing date with ISO
SY Scl	1450	1430	00 07 36.2	-25 34 16.1	39.5	80.1	07/12/96
IRAS 00193	1680	1630	00 21 47.3	-40 21 52.8	325.9	-75.4	11/11/96
IRC +10401	1010	15	19 03 18.2	+07 35 27.2	41.0	0.8	21/09/96
IRC -20540	1300	310	19 08 55.0	-22 18 56.4	14.6	-13.6	26/04/97
IRC -10502	840	150	19 20 18.1	-08 06 49.5	28.9	-10.1	25/10/96
AFGL 2392	2000	160	19 27 13.9	+07 08 56.4	43.4	-4.6	02/10/96
μ Cep	830	65	21 43 30.2	+58 51 25.4	100.6	4.4	03/03/97
IRAS 22231	1650	1370	22 26 10.7	-45 18 48.2	351.0	-55.9	03/06/96
IRC +10523	780	545	22 54 11.3	+08 58 44.7	80.6	-44.1	22/11/96
AFGL 3099	1500	1100	23 28 17.5	+10 59 13.9	92.3	-46.9	06/01/97
R Aqr	215	200	23 43 49.2	-15 21 43.7	66.3	-70.4	04/06/96

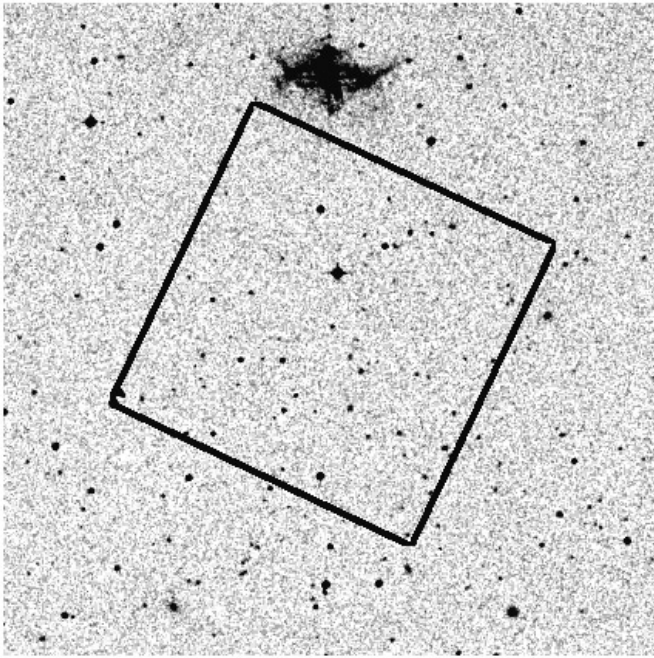


Fig. 3. Field from the Digital Sky Survey (R plate) of $12' \times 12'$. North is up and East, to the left. The bright object in the top is R Aqr with its optical nebula. The black line delineates the ISO field shown in Figs. 1 and 2

due to the loss of data. However, the visual inspection reveals a gradient and some structure.

The fluxes at 60 and 90 μm are generally well correlated. This is well seen in the individual maps. Although somewhat blurred by the averaging process, the correlation stays visible in the radial profiles (see Fig. 4).

4. Discussion

4.1. Interstellar or circumstellar origin

Extended IRAS emission has been observed around several late-type stars and commonly interpreted as due to a resolved

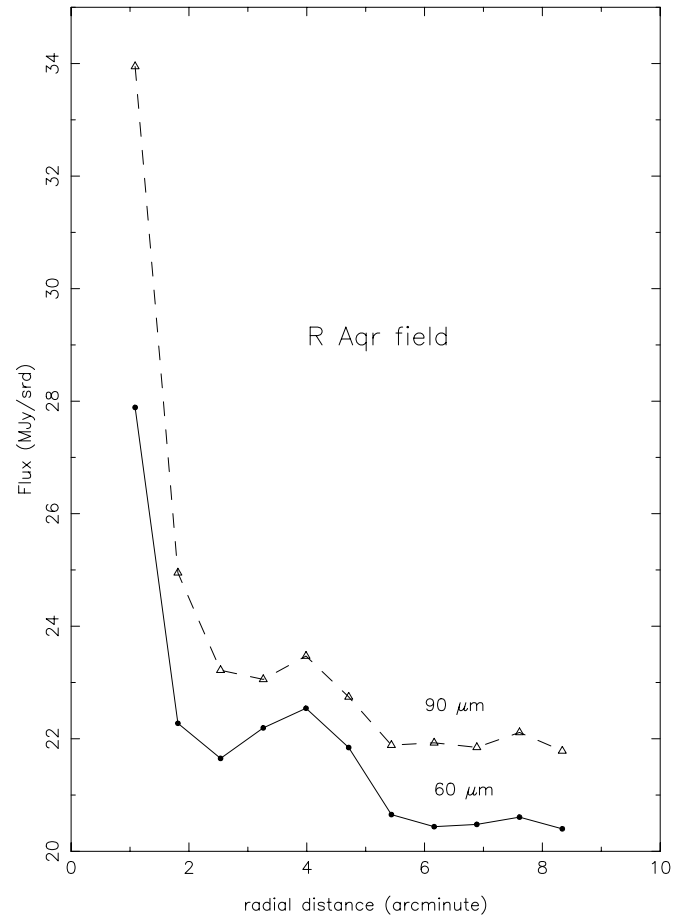


Fig. 4. Radial profile (with respect to the star) of the emission in the field near R Aqr; continuous line: 60 μm , dashed line: 90 μm . For clarity, the 90 μm profile has been shifted upwards by one unit. One notes the good correlation between the 60 and the 90 μm profiles. The horizontal scale is the distance from the heating source (kept outside the map) in arcminutes; at 215 pc, one arcminute translates to 0.06 pc

circumstellar shell (e.g. Young et al. 1993a). However, it is difficult to a priori decide between a circumstellar and an interstellar

Table 2. Results

AGB heating source	$\langle L \rangle$ $10^4 L_{\odot}$	size of the field (pc)	detection of a gradient
SY Scl	0.87	2.85	no
IRAS 00193	1.37	3.30	yes
IRC +10401	0.90	2.00	yes
IRC -20540	1.09	2.55	no
IRC -10502	1.06	1.65	yes
AFGL 2392	0.76	3.95	yes
μ Cep	40.	1.65	yes
IRAS 22231	0.91	3.24	no
IRC +10523	0.94	1.55	no
AFGL 3099	0.75	2.95	probably
R Aqr	0.80	0.40	yes

origin to this emission. Le Sidaner & Le Bertre (1993) argued that, in typical cases of AGB stars and assuming a circumstellar envelope with a density law $\propto 1/r^2$, the ISM density should dominate the circumstellar density at distances ≥ 0.5 pc from the star.

However, there are cases in which the $1/r^2$ law is probably incorrect. In the case of the C-rich AGB star U Hya, the extended emission has been studied in detail by Waters et al. (1994). It is seen as a ring of radius $\sim 1.5'$ (i.e. 0.2 pc at 350 pc). If the emission is due to circumstellar matter, it implies that, 10^4 years ago, the mass loss rate was a factor 25 higher than presently. In this case, an argument in favor of the circumstellar origin is the complete circular symmetry of the emission structure around the central source. Another case is discussed by Izumiura et al. (1996) who found with *ISO* a similar extended emission around Y CVn (radius $\sim 3'$, or 0.25 pc at 250 pc). In that case, the mass loss rate would have been, 10^4 years ago, a factor 100 larger than today. The evolutionary status of Y CVn is unclear, but it is worth noting that like U Hya it is also a C-rich Semi-Regular variable of type SRb. There is a converging body of evidence (e.g. Olofsson et al. 1992, Fouqué et al. 1992) suggesting that SRb variables have undergone recently a drastic decrease of their mass loss rate. On the other hand, apart from μ Cep, the sources in our sample are Miras for which such a recent event appears less probable.

Although only a small fraction of AGB stars are expected to possess bubbles of circumstellar matter like those of U Hya and Y CVn, and as our sample is small, it will be safer to examine carefully each individual case. In the following section, we detail the case of R Aqr whose proximity favors the detection of circumstellar matter.

4.2. R Aqr field

R Aqr is a symbiotic system consisting of a mass losing O-rich Mira of period 396 days and of a compact companion accreting part of the matter lost from the primary via an accretion disk (Whitelock 1987). Using the Period-Luminosity relation for O-rich Miras determined by Feast (1996), Le Bertre & Winters

(1998) derive a luminosity of $8 \cdot 10^3 L_{\odot}$ and estimate the distance to 215 pc. At this distance, the pixel in the map corresponds to 0.045 pc (Figs. 1 and 2) and the field center is at 0.29 pc from the star.

R Aqr is the nearest source in our sample. Its distance is comparable to those of U Hya (350 pc) and Y CVn (250 pc) for which extended circumstellar emissions have been reported (see above). In this unfavorable case, we might detect an extended emission of circumstellar origin. However, Young et al. (1993b) did not resolve its IRAS emission whereas they had very clearly detected the structures around Y CVn and U Hya. R Aqr is known to be surrounded by a $1' \times 2'$ optical nebula (Solf & Ulrich 1985), but this nebula is clearly out of the *ISO* field (Fig. 3).

The emissions at $60 \mu\text{m}$ and at $90 \mu\text{m}$ are clearly patchy. The peak in the profiles of Fig. 4 is due to the emission seen in the right edge of the maps near the star, and the bump at $4'$ is due mainly to the emission in the upper edge of the maps. The former might be of circumstellar origin, but the latter is more likely interstellar because in the IR maps there is no evidence of a ring structure nor of any connection with the optical nebulosity. It appears as a ~ 0.1 pc blob of IS matter heated by the red giant.

4.3. Comparison with other work

Murthy et al. (1992) have made a comparable search for ISM heated by stars in the IRAS data. They examined the volumes around 745 early-type (from O to G) stars and found an effect in 106 cases. Dring et al. (1996) reanalyzed the same data with an improved processing, and found an effect in 138 fields. From these two studies the incidence is ~ 0.15 – 0.20 . In contrast, Gaustad & Van Buren (1993) examined the IRAS data around ~ 1800 O6–B9.5 stars and found an incidence of ~ 0.35 .

At the present stage, the number of fields that we have examined is small, but the incidence in our sample seems to be ~ 0.5 – 0.6 . This is larger than found by Murthy et al. (1992) and Dring et al. (1996), and may be also larger than found by Gaustad & Van Buren (1993). With our observing strategy we probe only a part of the surroundings ($< 1/2$). So, the rate that we find tends to be underestimated. On the other hand, Gaustad & Van Buren and Dring et al. probe the ISM at distances up to 500 pc from the Sun, whereas our sources are in general at larger distances. It has been claimed that the Solar Neighborhood is devoid of IS matter. Also, it is noteworthy that O6–B9.5 stars range in luminosity from $\sim 10^5$ to $100 L_{\odot}$. Setting apart μ Cep, the range of luminosity of our sources is more restricted (from 0.7 to $1.4 \cdot 10^4 L_{\odot}$). Finally, the total volume probed by these authors is $\sim 5 \cdot 10^5 \text{ pc}^3$ whereas the volume that we have probed is only $\sim 200 \text{ pc}^3$.

In conclusion, differences and peculiarities are present in each approach and should be taken into account in a more thorough comparison. The main advantage of the *ISO* observations resides in the improved spatial resolution, $\sim 1'$ versus $6'$ for the IRAS Skyflux plates. We have noted on the images of several fields that the dust presents some structure on scales in the range 0.1–0.3 pc. Furthermore, as AGB stars are luminous evolved ob-

jects (with initial masses down to $\sim 1 M_{\odot}$), they are useful to probe the ISM far from the galactic plane: for instance, using IRAS 00193 allows detection of ISM dust at $z \sim 1600$ pc.

5. Conclusion

We have reported on observations obtained with *ISO* concerning 11 fields in the neighborhoods of luminous red giants. The data confirm that heating of the ISM by this kind of sources is locally important. Emission can be detected on nearby fields ($d \leq 2$ kpc) at $\lambda \sim 50\text{--}100 \mu\text{m}$ with the spatial resolution and sensitivity of *ISOPHOT*.

In this pilot study, we detect the effect in half of the cases. Although our sample is presently very small, the rate of occurrence appears higher than in previous studies based on IRAS data. A more complete survey is required to improve the statistics. Also, an improved absolute flux calibration would allow to intercompare the 60 and 90 μm images of each field and to evaluate the dust color temperature.

Acknowledgements. We are grateful to the *ISO* and *ISOPHOT* project members, and especially to R. Laureijs and T. Prusti for their advices on observing with *PHOT* and on data processing. This study has been financially supported by the CNRS programs “*ISO*” and “Physico-Chimie du Milieu Interstellaire” (PCMI).

References

- Désert F.-X., Boulanger F., Puget J.L., 1990, *A&A* 237, 215
 Dring A.R., Murthy J., Henry R.C., Walker H.J., 1996, *ApJ* 457, 764
 Feast M.W., 1996, *MNRAS* 278, 11
 Fouqué P., Le Bertre T., Epchtein N., Guglielmo F., Kerschbaum F., 1992, *A&AS* 93, 151
 Gaustad J.E., Van Buren D., 1993, *PASP* 105, 1127
 Humphreys R., 1978, *ApJSS* 38, 309
 Izumiura H., Hashimoto O., Kawara K., Yamamura I., Waters L.B.F.M., 1996, *A&A* 315, L221
 Kessler M.F., Steinz J.A., Anderegg M.E., et al., 1996, *A&A* 315, L27
 Le Bertre T., 1992, *A&AS* 94, 377
 Le Bertre T., 1993, *A&AS* 97, 729
 Le Bertre T., 1997, *A&A* 324, 1059
 Le Bertre T., Winters J.M., 1998, *A&A* 334, 173
 Lemke D., Klaas U., Abolins J., et al., 1996, *A&A* 315, L64
 Le Sidaner P., Le Bertre T., 1993, *A&A* 278, 167
 Murthy J., Walker H.J., Henry R.C., 1992, *ApJ* 401, 574
 Olofsson H., Carlström U., Eriksson K., Gustafsson B., 1992, *A&A* 253, L17
 Solf J., Ulrich H., 1985, *A&A* 148, 274
 Waters L.B.F.M., Loup C., Kester D.J.M., Bontekoe Tj.R., de Jong T., 1994, *A&A* 281, L1
 Whitelock P.A., 1987, *PASP* 99, 573
 Young K., Phillips T.G., Knapp G.R., 1993a, *ApJ* 409, 725
 Young K., Phillips T.G., Knapp G.R., 1993b, *ApJS* 86, 517